International Journal of Heat and Mass Transfer 123 (2018) 1212–1220

Contents lists available at ScienceDirect

International Journal of Heat and Mass Transfer

journal homepage: www.elsevier.com/locate/ijhmt

Effective thermal conductivity of packed bed adsorbers: Part 2 — Theoretical model

Mina Rouhani, Majid Bahrami *

Laboratory for Alternative Energy Conversion (LAEC), School of Mechatronic Systems Engineering, Simon Fraser University, BC V3T0A3, Canada

ARTICLE INFO

Article history:
Received 5 July 2017
Received in revised form 16 December 2017
Accepted 31 January 2018
Available online 16 February 2018

Keywords:
Effective thermal conductivity
Thermal contact resistance
Theoretical model
AQSOA FAM-Z02
Adsorption thermal energy storage
Young's modulus

ABSTRACT

In this study, a new comprehensive model is developed that can predict the effective thermal conductivity and thermal contact resistance of the packed bed adsorbers, as a function of water uptake, number of adsorbent layers, particle size, bed porosity, temperature, contact pressure, and gas pressure. The proposed model is successfully validated against experimental data for AQSOA FAM-Z02, measured by a heat flow meter. The relative differences of the experimental data and predicted values for the packed bed effective thermal conductivity are 2% and 3% at 25 and 80 °C, respectively. By increasing the water uptake from 0 to 0.3 kg kg_{ads}^{-1}, effective thermal conductivity of a 2 mm FAM-Z02 randomly packed bed is predicted to increase by 17% for temperature of 25 °C and 18% for temperature of 80 °C.

1. Introduction

Heating and cooling demands account for 60% of energy demand in the residential buildings [1], which are mainly supplied by conventional fossil fuels [2]. The use of renewables can lead to a significant reduction in fossil fuel consumption and greenhouse gas emissions. Thermal energy storage (TES) is an effective solution for exploiting heat sources with intermittent nature, i.e. renewables and waste heat. High energy storage density, low heat loss and using non-toxic and non-polluting refrigerants make adsorption TES (ATES) more appealing and effective for heat/cold storage, compared to the other thermal storage methods [3,4]. Packed bed adsorbers are widely used in adsorption cooling systems [5,6], adsorption dehumidification [7,8] and ATES [9,10], since they provide higher cooling/heating energy per volume compared to the adsorber beds with coated or consolidated adsorbent materials [11]. However, the low thermal conductivity of adsorbent materials, 0.1–0.8 W m^{-1} K^{-1} [12], and high thermal contact resistance (TCR) between the adsorbent particles and adsorber bed metal surfaces suppress the overall performance and reduce the competitiveness of the available packed bed adsorption systems.

To investigate and optimize the heat transfer performance of a packed bed adsorber, effective thermal conductivity of the packed bed adsorber as well as TCR should be measured and modeled properly. Although thermal conductivity measurement of adsorbent packed beds offers the possibility of realistically analyzing their thermal performances, it is costly and difficult to run the thermal conductivity measurement in large-scale for varying particle size, number of layers, filling gas pressure, relative humidity, contact pressure, water uptake, and temperature. Therefore, a comprehensive model for the packed bed effective thermal conductivity is vital to accurately analyze, predict, and improve the thermal performance of a packed bed adsorber.

Although importance of TCR has been raised in the literature [13–15], little has been shown regarding the modeling of TCR inside the adsorber bed. To consider the effect of TCR in the thermal conductivity calculations, the measured TCR from the available experimental data was fed into the theoretical models, in the literature [16,17]. Rezk et al. [17] presented a lumped analytical model for thermal conductivity of a silica gel packed bed and they applied a correlation fitted to the measured TCR, reported in Ref. [18], to their model.

The first type of effective thermal conductivity models is based on the analytical or numerical solutions to the Laplace's equation [19]. Maxwell analytical solution, which is based on the assumption of no thermal influence between individual particles, falls in this category [19]. On the other hand, numerical models of packed bed thermal conductivity, which do not need such limiting assumptions, suffer from high computational cost and time.

Introducing thermal resistance network for the packed bed adsorber is another type of solutions for modeling the effective

* Corresponding author.
E-mail addresses: mrouhani@sfu.ca (M. Rouhani), mbahrami@sfu.ca (M. Bahrami).

https://doi.org/10.1016/j.ijheatmasstransfer.2018.01.143

Nomenclature

A	surface area of the packed bed, m^2
ATES	adsorption thermal energy storage
a_L	radius of microcontact, mm
α_T	thermal accommodation coefficient
β	volume fraction
d	adsorbent particle diameter, mm
δ	displacement, mm
ε	adsorbent particle porosity
E	Young's modulus, GPa
F	contact force, N
FCC	face center cubic arrangement
k	thermal conductivity, $W\,m^{-1}\,K^{-1}$
k_{tot}	packed bed total thermal conductivity (effects of TCR is included), $W\,m^{-1}\,K^{-1}$
$k_{eff,bed}$	packed bed effective (medium) thermal conductivity (effects of TCR is not included), $W\,m^{-1}\,K^{-1}$
L	packed bed length (thickness), mm
m	number of adsorbent particles in each adsorbent layer
n	number of layers of adsorbent particles
r	adsorbent particle radius, mm
ν	Poisson's ratio
ω	water uptake, $kg\,kg_{ads}^{-1}$
P	gas pressure, Pa
P_{sat}	saturation pressure at adsorbent temperature, Pa
$P_{contact}$	contact pressure at the contact of adsorbent particle and the metal surface, Pa
$\dot{Q}_{g,micro}$	micro-gap heat flow, W
$\dot{Q}_{G,macro}$	macro-gap heat flow, W
$\dot{Q}_{C,macro}$	macro-contact heat flow, W
$\dot{Q}_{c,micro}$	micro-contact heat flow, W
R	thermal resistance, $K\,W^{-1}$
SC	simple cubic arrangement
ψ	packed bed solid fraction
T	temperature, K
TCR	thermal contact resistance, $K\,W^{-1}$

Subscripts

bed	packed bed
cell	cell
contact	at the contact of adsorbent particles and the heat exchanger metal surface
eff	effective
g	adsorbate gas
p	adsorbent particle
s	solid particle (adsorbent skeleton)
tot	total
w	water
wet	wet adsorbent particle

thermal conductivity of the packed bed adsorbers [19]. Griensinger et al. [20] experimentally and theoretically studied the effective thermal conductivity of zeolite powder, introducing three main parallel heat transfer paths: pure solid, pure fluid, and mixed solid-fluid paths. They defined tuning parameters by fitting the theoretical curve to the measured values [20]. Similarly, Dawoud et al. [21] developed a model to calculate the effective thermal conductivity of wetted zeolite 4A, assuming an isotropic distribution of adsorbed water inside the zeolite crystal. They introduced a tortuosity factor for conductive heat transfer and their model took into account the Knudsen conductivity of the vapor phase through the curve fittings to their experimental data [21]. Nevertheless, thermal conductivity models of small amount of adsorbent sample, i.e. an adsorbent particle or powder, cannot be a good representative of a large-scale packed bed adsorber, since they do not take into account all the thermal resistances inside the packed bed, including the thermal resistance between the adsorbent particles as well as TCR.

Another type of effective thermal conductivity models is based on calculating thermal conductivity of a unit cell (as a representative of the repeating units in a packed bed), using thermal resistance network or basic models such as Maxwell. Luikov et al. [22] defined a thermal resistance circuit for an elementary cell, containing a solid skeleton and the surrounding gas. The boundary unit cell and water uptake were not considered in their study [22]. In addition to their model, Sarwar and Majumdar [23] took into account the effects of the water content on thermal conductivity of the packed bed adsorbers, although interstitial gas pressure and the contact pressure were not considered as variables in this model [23].

In this work, a new comprehensive analytical unit-cell model is developed to predict effective thermal conductivity of a packed bed adsorber as a function of numbers of adsorbent layers, adsorbent properties, particle size, water uptake, temperature, contact pressure, roughness, particle arrangement, and gas pressure. TCR is also taken into account in the calculation of the total thermal conductivity of the packed bed adsorbers. Young's modulus of a 2-mm diameter AQSOA FAM-Z02 particle is also measured for the first time and used in this model. This model is applicable to both open and closed adsorption systems and provides a platform for a comparison of thermal performance between open and closed packed bed adsorber under various conditions. The present model is validated with the experimental data, collected by heat flow meter method.

2. Present model

Modeling of effective thermal conductivity of a packed bed adsorber consists of two main parts: (1) modeling the effective thermal conductivity of an adsorbent particle, taking account of adsorbent water content, and (2) modeling the effective thermal conductivity of the packed bed adsorber. It is assumed that the steady state condition was reached for both temperature and uptake. Therefore, the uptake of the adsorbent particles is corresponded to the equilibrium water uptake at steady-state temperature and relative humidity (or pressure ratio, P/P_{sat}, for the closed adsorption systems).

Since natural convection in the small voids between the adsorbents can be neglected [24], and in both model and experimental data, the heat flow is downward to eliminate the natural convection [25,26], and radiation is negligible in the packed beds at low temperatures (below 600 °C [27]), heat transfer occurs via conduction through solid adsorbent and conduction through the interstitial gas. These conductive heat transfer mechanisms take place in macroscale and microscale levels. Fig. 1 shows the macro-contact, $Q_{C,macro}$, micro-contact, $Q_{c,micro}$, macro-gap, $Q_{G,macro}$, and micro-gap, $Q_{g,micro}$, heat flow lines, for simple cubic (SC) arranged packed bed.

2.1. Effective thermal conductivity of a packed bed adsorber

In this study, thermal conductivity modeling of a packed bed is performed based on the unit cell approach, where thermal conductivity calculation is made for an elementary cell, shown in Fig. 2a,

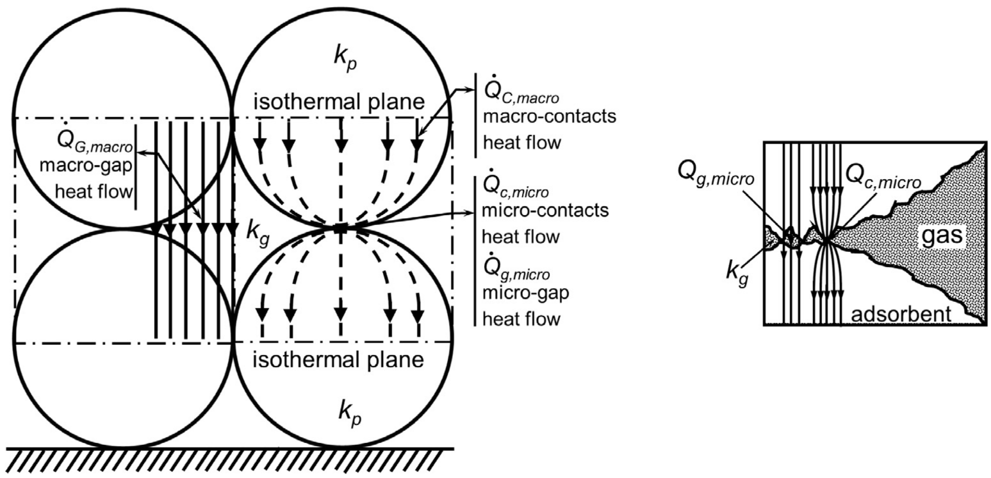

Fig. 1. Heat conduction in a packed bed adsorber, including: (i) macro-contact heat flow, $\dot{Q}_{C,macro}$, (ii) macro-gap heat flow, $\dot{Q}_{G,macro}$, (iii) micro-contact heat flow, $\dot{Q}_{c,micro}$ and (iv) micro-gap heat flow, $\dot{Q}_{g,micro}$.

as a representative of the entire packed bed medium. It is assumed that the heat conduction in the unit cell is one dimensional, which leads to isothermal top and bottom surfaces while the lateral walls are adiabatic due to symmetry [28]. Fig. 2b illustrates the unit cell and the associated thermal resistance network. The thermal resistance of a unit cell consists of: (1) bulk thermal resistance of particles, R_p, (2) macro-contact constriction/spreading resistance, $R_{C,macro}$, (3) microcontact constriction/spreading resistance, $R_{c,micro}$, (4) resistance of the interstitial gas in the micro-gap, $R_{g,micro}$, and (5) resistance of interstitial gas in the macro-gap, $R_{G,macro}$.

Bahrami et al. [28] developed compact analytical models to predict the micro/macro constriction/spreading and micro/macro-gap resistances in packed beds of high conductive particles (i.e. particle thermal resistance was much less than the gas resistance). In the present study, their analytical solutions are followed, as a platform for dry adsorber bed, while particle thermal resistance is also considered, and afterwards extended for the thermal conductivity of wet adsorber bed, considering the adsorbent particle water uptake. The equations used in this study are presented in Appendix A, and more details are found in Ref. [28].

These micro and macro thermal resistances depend on the thermal and physical properties of the adsorbent material, including thermal accommodation, $\alpha_{T,p}$, and Young's modulus, E_p (see Appendix A). Few information is available concerning the properties of AQSOA FAM-Z02. Table 1 provides the specifications of FAM-Z02, reported in the literature. Thermal accommodation, which represents the energy exchange process through gas-surface collision, affects both macro-gap and micro-gap resistances (see Appendix A). Adsorption can increase the thermal accommodation up to 5 times, compared to the clean surfaces [29] and α_T can reach higher than 1 [30]. The thermal accommodation coefficient of zeolite was considered 1.95, as a fitting parameter in Ref. [21]. Here, assuming a clean surface for the adsorbent, a correlation for thermal accommodation of clean surfaces, which is developed by Song and Yovanovich [29], is used (see Eq. (A24) in Appendix A).

Particle contact resistance depends on the Young's modulus of adsorbent material. A thermomechanical analyzer (TMA Q400EM from TA Instruments), shown in Fig. 3a, with precision of ±0.1% was used to measure the Young's modulus of the adsorbent particle. As shown in Fig. 3a, a 2-mm diameter FAM-Z02 particle was compressed with linear ramp force up to 1 N in a dry nitrogen environment at room temperature, between the quartz glass sample stage and macro-expansion probe with a 6.07 mm diameter contact area. The value of $0.5736\ \mathrm{GPa}^{-1}$ was obtained for $(1-\nu_p^2)/E_p$ (see Fig. 3b). Assuming a value of 0.3 for Poisson ratio, the Young modulus of FAM-Z02 was 1.59 GPa.

Using the unit cell thermal resistance network, shown in Fig. 2b, the total thermal resistance of the unit cell is obtained by:

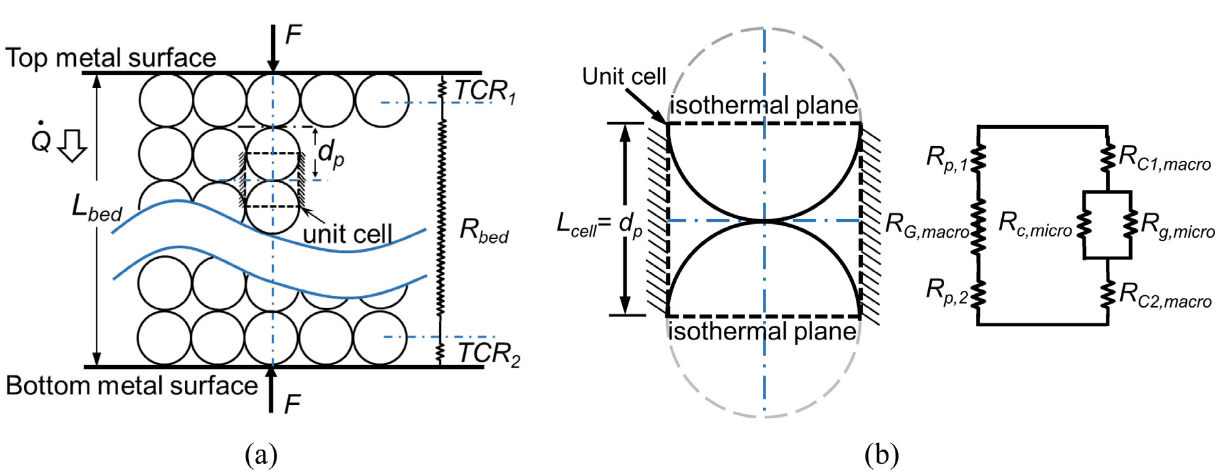

Fig. 2. (a) Packed bed adsorber of adsorbents with diameter of d_p, for simple cubic (SC) arrangement [28] and (b) a unit cell of the SC-arranged adsorber bed with the equivalent electrical circuit.

Table 1
Specifications of AQSOA FAM-Z02.

Material	FAM-Z02	
Provider	Mitsubishi Plastic Inc.	
Chemical formula	$Al_{0.56}Si_{0.02}P_{0.42}O_2$	[31]
Structure IZA code	SAPO34 CHA	[32]
Differential heat of adsorption, kJ kg_w^{-1}	3240 (298 K)	[33]
Bulk density, kg m^{-3}	0.6–0.7	[33]
Specific heat, J kg^{-1} K^{-1}	0.822 (303 K)	
	0.942 (363 K)	[33]
Thermal conductivity, W m^{-1} K^{-1}	0.117 (303 K)	
	0.128 (363 K)	[33]
Particle diameter, mm	0.1–2	[33]
Pore diameter, Å	3.8	[32]
BET surface area, m^2 g^{-1}	590	[31]
	717.8	[34]
Pore volume, cm^3 g^{-1}	0.2769	[31]
	0.27	[34]

$$R_{cell} = \left[\frac{1}{(1/R_{c,micro} + 1/R_{g,micro})^{-1} + R_{C,macro}} + \frac{1}{R_p + R_{G,macro}}\right]^{-1} \quad (1)$$

The effective thermal conductivity of each cell can be found by $k_{eff,cell} = L_{cell}/(R_{cell}A_{cell})$, which is also the effective thermal conductivity of the packed bed, $k_{eff,bed}$, considering a homogenous medium. Number of unit cells in each layer of a SC-arranged adsorber bed is equal to the number of adsorbent particles in the layer, m. Thermal resistances of the unit cells along the length of bed (i.e. in the heat transfer direction) are in series, while they are parallel to each other in the direction perpendicular to the heat transfer path. Thus, the thermal resistance of the adsorber medium is $R_{bed} = [L_{bed}/(k_{eff,bed}A_{cell})]/m$, where L_{bed} is the bed length in the heat transfer direction.

The TCR in the unit cells adjacent to the two metal surfaces of heat exchanger medium, are also in series with the medium resistance (R_{bed}). Thus, the total bed resistance is $R_{tot} = R_{bed} + TCR$. To this end, the total thermal conductivity of a dry packed bed can be found from:

$$k_{tot} = \frac{L_{bed}}{A(R_{bed} + TCR)} \quad (2)$$

where $A = m\,A_{cell}$ is the total area of the metal surface.

Similarly, all the thermal resistances in the adsorbent particle and the gas are calculated for the face center cubic (FCC) arrangement, using related equations in Ref. [28] and the parameters in Table 2, for FCC arrangement.

2.2. Effective thermal conductivity of an adsorbent particle

Effective thermal conductivity of an adsorbent particle is influenced by thermal conductivities of the solid adsorbent, adsorbed water and the filling gas inside the pores of adsorbent particle. Fig. 4a and b show schematics of a wet adsorbent and the unit cell for a wet SC-arranged packed bed adsorber. The above-mentioned model for the dry packed beds can be extended to account for the heat transfer through the adsorbed water. A wet adsorbent is an inhomogeneous medium of three components: (i) solid particle (adsorbent skeleton), (ii) adsorbed water on the surface of adsorbent pores and (iii) interstitial gas, which is air in open adsorption system and water vapor in the closed adsorption system.

Having been treated as a homogeneous medium, the wet adsorbent particles are modeled by the effective-medium approximation (EMA). Among various models of EMA, Bruggeman's method for multi-component medium is selected, since it is applicable to arbitrary volume fractions [35]. Therefore, the effective thermal conductivity of a wet adsorbent particle, $k_{p,wet}$, can be calculated as follows,

$$\sum_{i=1}^{3}\beta_i \frac{k_i - k_{p,wet}}{k_i + 2k_{p,wet}} = 0, \quad \text{where} \quad \sum_{i=1}^{3}\beta_i = 1 \quad (3)$$

where β_i is the volume fraction of each component. Volume fraction of solid particle, water and gas are obtained from Eq. (4).

$$\beta_s = 1 - \varepsilon$$
$$\beta_w = \omega \frac{\rho_s}{\rho_w}(1 - \varepsilon) \quad (4)$$
$$\beta_g = \varepsilon - \omega \frac{\rho_s}{\rho_w}(1 - \varepsilon)$$

where ε is the porosity of the adsorbent particle and ρ_s is the poreless density of the adsorbent material.

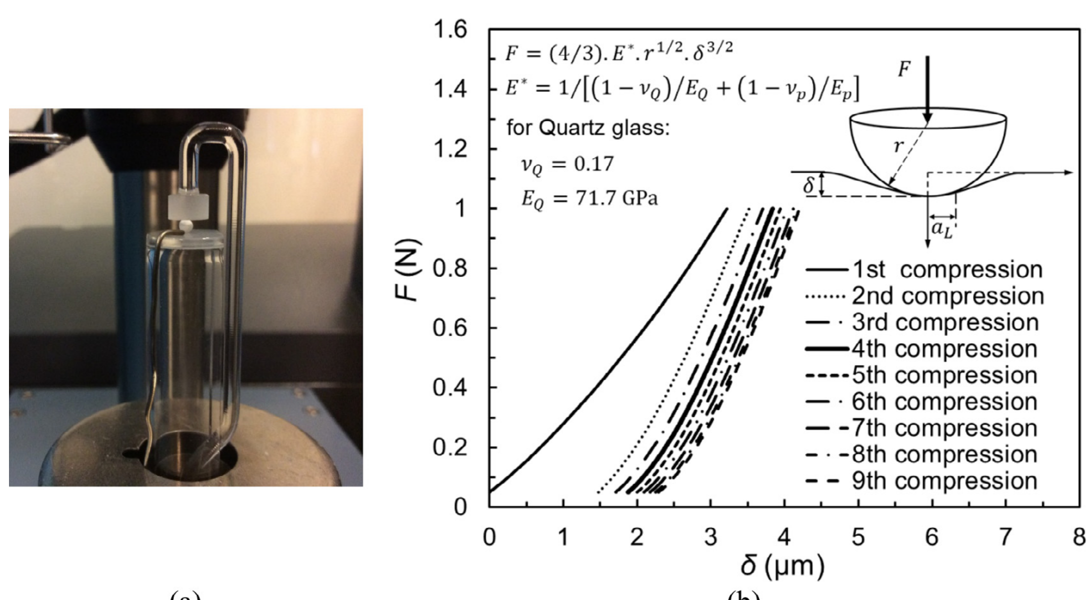

Fig. 3. (a) Thermomechanical analyzer (TMA Q400EM from TA Instruments) and a AQSOA FAM-Z02 particle placed between quartz glass sample stage and macro-expansion probe and (b) the force applied on the adsorbent particle versus half-displacement of the adsorbent particle at 25 °C.

Table 2
Specifications of SC and FCC arrangements of packed bed.

Packing arrangement	Solid fraction, ψ_{bed}	Bed length, L_{bed}	Cell area, A_{cell}	Cell length, L_{cell}	Boundary cell length, L_{b-cell}
SC	0.524	$n \times d_p$	d_p^2	d_p	$d_p/2$
FCC	0.740	$((n-1)\sqrt{2}/2+1) \times d_p$	$d_p^2/2$	$\sqrt{2}d_p/2$	$d_p/2$

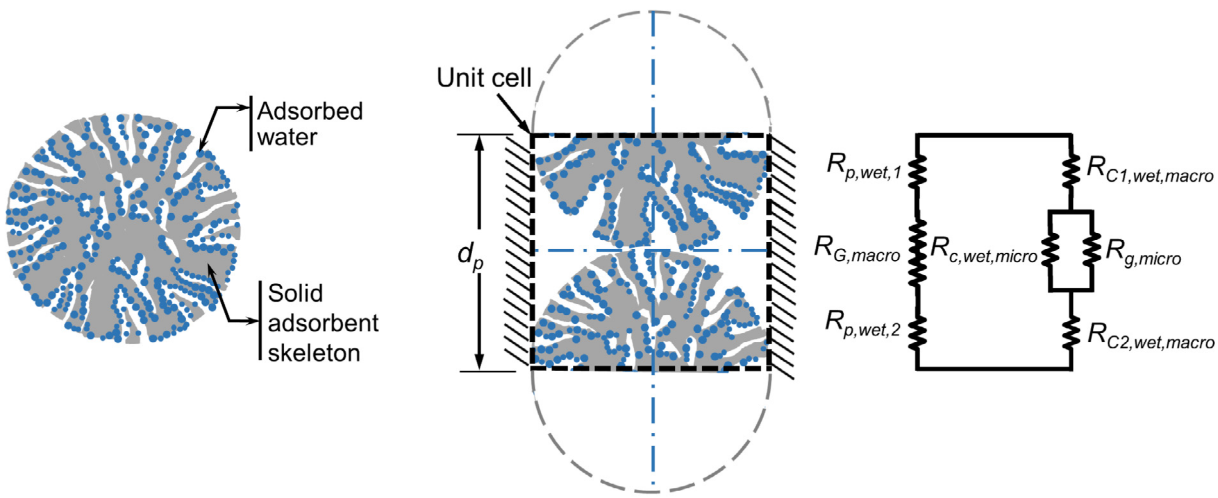

Fig. 4. (a) Schematic diagram of a wet adsorbent and (b) a unit cell for a SC-arranged wet packed bed adsorber with the equivalent electric circuit.

When the thermal conductivity measurement of the dry adsorbent particle is done in atmospheric condition and the reported thermal conductivity of adsorbent also includes the effects of the thermal conductivity of gas (air), two components (i = 2) can be considered: (i) adsorbed water, with the volume fraction of $\omega \frac{\rho_s}{\rho_w}(1-\varepsilon)$ and (ii) a combination of air and solid adsorbent, with volume fraction of $1-\omega \frac{\rho_s}{\rho_w}(1-\varepsilon)$.

The effective thermal conductivity of the wet adsorbent particle, $k_{p,wet}$, which is calculated from Eq. (3), should be plugged into Eqs. (A2), (A3) and (A6), to calculate micro-contact ($R_{c,micro,wet}$) and macro-contact ($R_{C,macro,wet}$) resistances, and consequently the effective thermal conductivity of the wet packed bed, $k_{eff,bed,wet}$.

2.3. Asymptotic solution for intermediate solid fraction (randomly) packed bed adsorber

The effective thermal conductivity of a randomly packed bed ($\psi_{bed} \approx 0.6$ [36]) falls between that of two arrangements: SC ($\psi_{bed} = 0.524$), as the lower bound, and FCC ($\psi_{bed} = 0.740$), as the upper bound [37,38]. Thus, the thermal conductivity obtained from the above-mentioned developed model for SC and FCC arrangements, as two limiting cases, can be blended to find the thermal conductivity of a randomly packed bed [38]. Assuming a linear dependence for the thermal conductivity versus the packed bed solid fraction, the following equation is applied for a randomly packed bed.

$$\frac{\psi_{bed} - \psi_{SC}}{\psi_{FCC} - \psi_{SC}} = \frac{k_{eff,bed} - k_{eff,SC}}{k_{eff,FCC} - k_{eff,SC}} \tag{5}$$

where ψ_{SC}, ψ_{FCC} and ψ_{bed} are the solid fractions of the SC, FCC and any randomly packed bed arrangements, respectively. ψ_{bed} for a randomly packed bed adsorber can be assumed about 0.62 (porosity of 0.38 [39]) or can be chosen such that $k_{eff,bed}$ approaches the experimental data collected for thermal conductivity of that randomly packed bed. This asymptotic solution is applicable for any packed bed adsorber with arbitrary solid fraction of ψ_{bed}. Thus, the present model is not limited by the bed arrangement, since it covers SC and FC arrangements as well as any randomly-arranged packed bed adsorber.

3. Results and discussion

The developed mathematical model, described in Section 2, is coded into MATLAB and consists of four main sections: (i) water uptake calculation, (ii) adsorbent particle thermal resistance, (iii) packed bed cell resistance and (iv) packed bed boundary cell resistance. Water uptake is calculated depending on the temperature

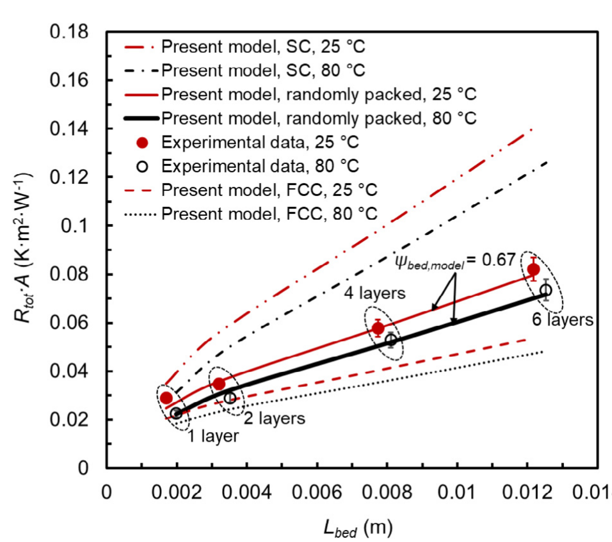

Fig. 5. $R_{tot} \cdot A$ versus bed thickness for 2-mm FAM-Z02 packed beds with water uptake of 0.30 ± 0.02 kg kg_{ads}^{-1} at temperatures of 25 and 80 °C and under contact pressures of 0.7 kPa, including experimental data and model results for SC, FCC and the randomly packed bed.

and relative humidity from the equilibrium isotherm of the adsorbent. The water uptake is fed to the "particle resistance" code, where the effective thermal conductivity of a wet particle is calculated. Having the effective thermal conductivity of the wet adsorbent particles, thermal resistances of the internal and boundary unit cells are calculated in the "packed bed cell resistance" and the "boundary cell resistance" sections, respectively.

Fig. 5 shows the $R_{tot} \cdot A$ of a FAM-Z02 packed bed adsorber versus the bed thickness (or number of adsorbent layers) at two temperatures, 25 and 80 °C. As previously mentioned, SC arrangement is the upper bound for thermal resistance (i.e. lower bound for the thermal conductivity), while FCC arrangement is the lower bound for thermal resistance (i.e. upper bound for thermal conductivity). The present model for solid fraction, ψ_{bed}, of 0.67, shows good agreement with the experimental data collected at 25 and 80 °C for two, four and six layers. The maximum relative difference is 16% for one layer, at 25 °C, where the share of the TCR in the total resistance is significant, i.e. 67% of the total resistance [40]. The present model captures the trend of the measured TCR in a qualitative comparison, however, the calculated TCR cannot be compared quantitatively with the measured TCR, due to the FAM-Z02 dust observed on the metal sheets, possible surface oxidation of the aluminum sheets, imperfect contact of the adsorbent and locally warped aluminum sheets.

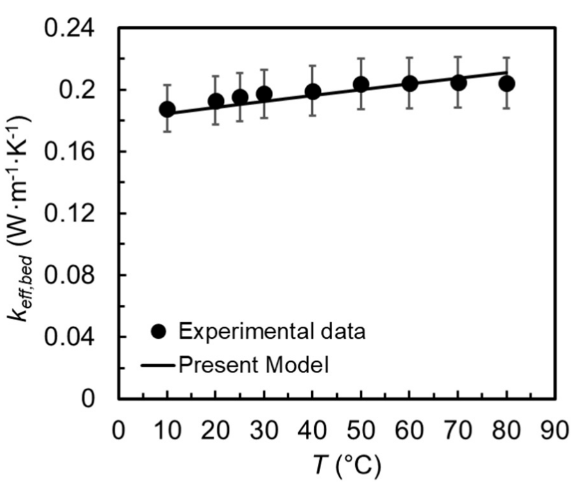

Fig. 6. Effective thermal conductivity versus mean temperature of a 2-mm FAM-Z02 randomly packed bed adsorber with water uptake of 0.30 ± 0.02 kg kg_{ads}^{-1} under contact pressure of 0.7 kPa, including the result from the present model for ψ_{bed} = 0.67 and experimental data [40].

To provide the effective bulk thermal conductivity of a packed bed adsorber, the effects of the TCR should be deconvoluted from the total thermal resistance of the packed bed, as discussed in Ref. [40]. Fig. 6 shows the effective thermal conductivity of the 2-mm diameter FAM-Z02 packed bed adsorber versus the mean temperature inside the bed, in which the effects of TCR is deconvoluted. Effective thermal conductivity of the FAM-Z02 randomly-packed bed adsorber varies between 0.188 and 0.204 W m^{-1} K^{-1}, and slightly increases with the increase in temperature. The present model can predict the $k_{eff,bed}$ accurately and the maximum relative difference between the results from model and experimental data is 3% at 80 °C.

Total thermal conductivity of the packed bed adsorber is shown in Fig. 7 for temperatures of 10–80 °C and various numbers of adsorbent layers. By increasing the temperature, total thermal conductivity increases because of a higher thermal conductivity of air and adsorbent at higher temperatures, and a better contact of adsorbent with the metal sheets and less TCR. As shown in Fig. 7, the model successfully predicts the total thermal conductivity; the maximum difference between the results of the model and the experimental data occurs for lower temperatures and at lower number of layers, where the effect of TCR on the total thermal conductivity is the highest. As the number of layers increases, the thermal behavior of the bed approaches an "effective" or continuum medium and thermal conductivity becomes independent of the number of layers. The present model shows that total thermal conductivities, k_{tot}, of 100 and 1000 adsorbent layers are close to one another, and approach the effective thermal conductivity of the packed bed medium, $k_{eff,bed}$, as shown in Fig. 7.

The effect of water uptake on the total thermal conductivity of 4-layer FAM-Z02 packed bed adsorber is shown in Fig. 8a. Total thermal conductivity of the randomly packed bed with uniform adsorbent water uptake of 0.3 kg kg_{ads}^{-1} is predicted to be 19–20% higher compared to an identical but completely dry bed, for the mean temperature range of 10–80 °C. On the other hand, the total thermal conductivity of a 4-layer FAM-Z02 packed bed at water uptake of 0.3 kg kg_{ads}^{-1} is predicted to increase 14%, when the mean temperature increases from 10 to 80 °C. As shown in Fig. 8b, effective thermal conductivity of the FAM-Z02 randomly packed bed is predicted to increase by 17% from 0.163 to 0.191 W m^{-1} K^{-1}, at 25 °C, and by 18% from 0.179 to 0.211 W m^{-1} K^{-1}, at 80 °C, when the water uptake increases from 0 to 0.3 kg kg_{ads}^{-1}.

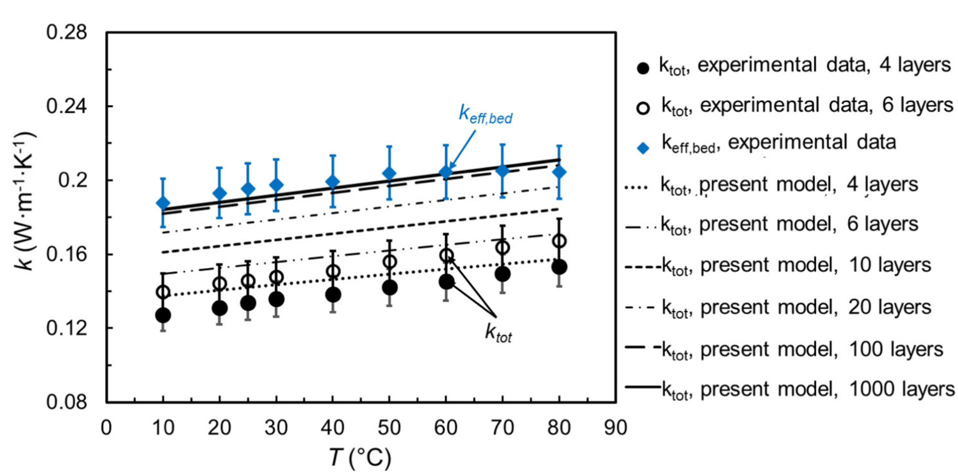

Fig. 7. Total thermal conductivity versus temperature for 2-mm FAM-Z02 packed bed adsorbers, with water uptake of 0.30 ± 0.02 kg kg_{ads}^{-1} and under contact pressure of 0.7 kPa, for various numbers of adsorbent layers (comparison between experimental data and the present model). For higher numbers of adsorbent layers, total thermal conductivity approaches the packed bed effective thermal conductivity.

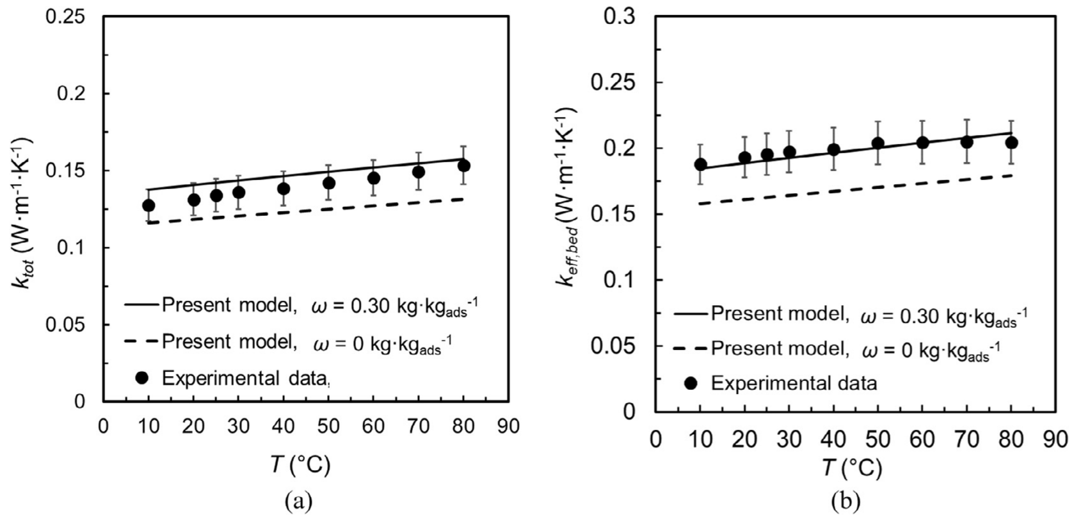

Fig. 8. Effect of water uptake change from 0 to 0.3 kg kg_{ads}^{-1} on the (a) total thermal conductivity of a 4-layer randomly packed bed and (b) effective thermal conductivity of the randomly packed bed adsorber, under contact pressure of 0.7 kPa.

Fig. 9 shows the effect of adsorbent diameter on the effective thermal conductivity of a SC-arranged packed bed of FAM-Z02, while the bed thickness is kept constant at 12 mm (i.e. number of adsorbent layers for 0.25 and 6 mm diameter particles are 48 and 2, respectively). As shown in Fig. 9, for a fixed bed length, packed bed of smaller adsorbent materials has higher thermal resistance and therefore lower thermal conductivity. However, decreasing the adsorbent size leads to an increase in the uptake rate and specific power (SP = averaged power/adsorbent mass) [41], which should be considered in the adsorbent size selection, as well.

Fig. 10 shows the effect of the thermal conductivity of the adsorbent particles on the effective thermal conductivity of a wet FAM-Z02 packed bed adsorber. Effective thermal conductivity of the packed bed is higher for higher adsorbent thermal conductivity, although the increase rate in the $k_{eff,bed}$ becomes slower when the thermal conductivity of the solid adsorbent particle passes 1 W m^{-1} K^{-1}. At high pressures (e.g. atmospheric pressure), the controlling conductance is the thermal conductivity of the interstitial gas. If thermal conductivity of the adsorbent particle increases to 100 W m^{-1} K^{-1}, effective thermal conductivity of the packed bed adsorber is predicted to be 0.51 W m^{-1} K^{-1} at 25 °C and 0.54 W m^{-1} K^{-1} at 80 °C, when water uptake is 0.3 kg kg_{ads}^{-1}. To this end, there is not much gain in improving the thermal conductivity of the adsorbent particle in the packed bed adsorber above 1 W m^{-1} K^{-1} for open (atmospheric) adsorption systems.

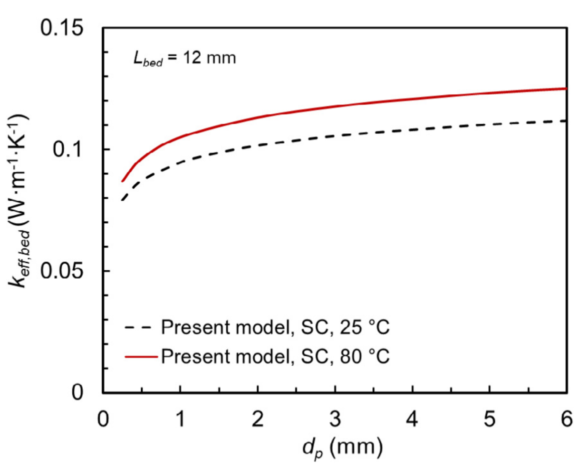

Fig. 9. Effect of particle diameter on the effective thermal conductivity of a SC-arranged packed bed of FAM-Z02 with water uptake of 0.3 kg kg_{ads}^{-1} at 25 and 80 °C and under contact pressure of 0.7 kPa. The bed thickness is fixed at 12 mm.

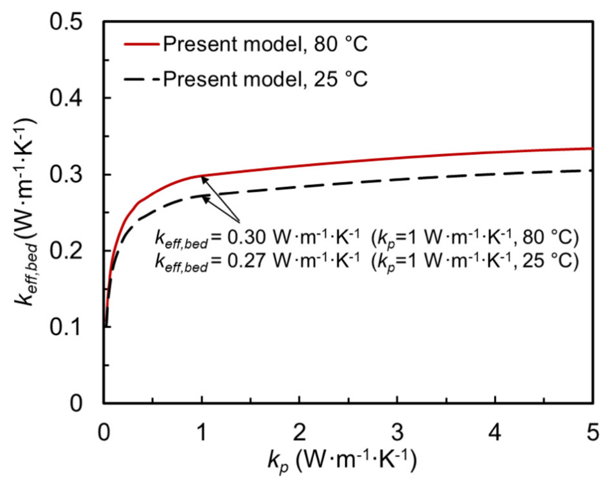

Fig. 10. Effect of the thermal conductivity of dry adsorbent on the effective thermal conductivity of 2-mm FAM-Z02 packed bed adsorber with water uptake of 0.3 kg kg_{ads}^{-1} and under contact pressure of 0.7 kPa.

4. Conclusions

In this study, a comprehensive model was developed to predict the effective thermal conductivity and TCR of a packed bed adsorber, as a function of water uptake, number of adsorbent layers, particle size, bed porosity, temperature, contact pressure, and gas pressure for SC, FCC, and any randomly packed bed. The model was applicable to both open and closed (vacuum) adsorption systems. The maximum relative difference of the experimental data and predicted value for the effective thermal conductivity of packed bed adsorber was 2% at 25 °C and 3% at 80 °C. A parametric study was conducted to evaluate the effects of the key parameters on the effective thermal conductivity of the packed bed adsorber. By increasing the water uptake from 0 to 0.3 kg kg_{ads}^{-1}, effective thermal conductivity of a FAM-Z02 randomly packed bed was predicted to increase by 17 and 18% for temperatures of 25 and 80 °C,

Table A1
Equations used to find the thermal resistance of the unit cell, R_{cell}, [28,29].

Equations		Eq. number	Ref.
$R_{cell} = \left[\frac{1}{(1/R_{c,micro}+1/R_{g,micro})^{-1}+R_{C,macro}} + \frac{1}{R_p+R_{G,macro}}\right]^{-1}$	$K\,W^{-1}$	A1	[28]
$R_{c,micro} = [0.565H_{mic}(\sigma_p/m_p)]/(k_sF)$	$K\,W^{-1}$	A2	[28]
$R_{C,macro} = 1/(2k_s a_{macro})$	$K\,W^{-1}$	A3	[28]
$R_{g,micro} = (2\sqrt{2}\sigma_p a_2)\Big/\left\{\pi k_g a_L^2 \ln\left(1+\frac{a_2}{a_1+M/[2\sqrt{2}\sigma_p]}\right)\right\}$	$K\,W^{-1}$	A4	[28]
$R_{G,macro} = \frac{2}{\pi k_g\left[S\ln\left(\frac{S-B}{S-A}\right)+B-A\right]}$	$K\,W^{-1}$	A5	[28]
$k_s = \frac{2k_{p,1}k_{p,2}}{k_{p,1}+k_{p,2}}$	$W\,m^{-1}\,K^{-1}$	A6	[28]
$H_{micro} = c_1(d_v/\sigma_0)^{c_2}$	Pa	A7	[28]
$\sigma_0 = 1\ \mu m$, $d_v = \sqrt{2\pi}a_{C,macro} = 0.95(\sigma_p/m_p)$	m	A8	[42]
$c_1 = H_{BGM}(4.0 - 5.77\kappa + 4.0\kappa^2 - 0.61\kappa^3)$, $\kappa = H_B/H_{BGM}$	Pa	A9	[28]
$c_2 = -0.57 + 0.82\kappa - 0.41\kappa^2 - 0.06\kappa^3$		A10	[28]
$H_{BGM} = 3.178$ GPa, $1.3 \leqslant H_B \leqslant 7.6$ GPa	Pa	A11	[28]
$m_p = \sqrt{m_{p1}^2 + m_{p2}^2}$, $m_{p1} = 0.076\sigma_{p1}^{0.52}$		A12	[28]
$\sigma_p = \sqrt{\sigma_{p1}^2 + \sigma_{p2}^2}$	m	A13	[28]
$\frac{a_{macro}}{a_H} = \begin{cases} 1.605/\sqrt{\acute{P}_0} & 0.01 \leqslant \acute{P}_0 \leqslant 0.47 \\ 3.51 - 2.51\acute{P}_0 & 0.47 \leqslant \acute{P}_0 \leqslant 1 \end{cases}$		A14	[28]
$\acute{P}_0 = P_0/P_{0,H} = 1/(1+1.37\alpha(\rho/a_H)^{-0.075})$, $\alpha = \frac{\sigma\rho}{a_H^2}$		A15	[28]
$P_{0,H} = 1.5F/(\pi a_H^2)$	Pa	A16	[28]
$a_H = (0.75F\rho/\acute{E})^{1/3}$	m	A17	[28]
$\acute{E} = \left[(1-v_{p1}^2)/E_{p1} + (1-v_{p2}^2)/E_{p2}\right]^{-1}$	Pa	A18	[28]
$\rho_p = (1/\rho_{p1} + 1/\rho_{p2})^{-1}$	m	A19	[28]
$a_1 = \mathrm{erfc}^{-1}(2P_0/\acute{H})$, $a_2 = \mathrm{erfc}^{-1}(0.003P_0/\acute{H}) - a_1$		A20	[28]
$\acute{H} = c_1(1.62(\sigma_p/\sigma_0)/m_p)^{c_2}$	GPa	A21	[28]
$M = \left(\frac{2-\alpha_{T1}}{\alpha_{T1}} + \frac{2-\alpha_{T2}}{\alpha_{T2}}\right)\left(\frac{2\gamma_g}{1+\gamma_g}\right)\frac{1}{Pr}\Lambda$	m	A22	[28]
$\Lambda = \frac{P_{ref}}{P_g}\frac{T_g}{T_{ref}}\Lambda_{ref}$,	m	A23	[28]
Λ_{ref}: mean free path value at reference gas temperature T_{ref} and pressure P_{ref}			
$\alpha_T = \exp\left[-0.57\left(\frac{T_s-T_{ref}}{T_{ref}}\right)\right]\left(\frac{M^*}{6.8+M^*}\right) + \frac{2.4\mu}{(1+\mu)^2}\left\{1-\exp\left[-0.57\left(\frac{T_s-T_{ref}}{T_{ref}}\right)\right]\right\}$,		A24	[29]
$\mu = M_g/M_s$			
$M^* = \begin{cases} M_g & \text{monoatomicgas} \\ 1.4M_g & \text{diatomic/polyatomicgas} \end{cases}$	$kg\,mol^{-1}$	A25	[29]
$A = 2\sqrt{\rho_p^2 - a_L^2}$, $B = 2\sqrt{\rho_p^2 - b_L^2}$, $S = 2(\rho-\omega_0)+M$, $\omega_0 = a_L^2/(2\rho)$	m	A26	[28]

respectively. At a constant bed thickness, effective thermal conductivity increased by increasing the adsorbent particle diameter, due to the less resistances between the adsorbent particles. Improving thermal conductivity of the solid adsorbent particle above 1 $W\,m^{-1}\,K^{-1}$, in an open system, was not worthy of consideration since it led to a minimal increase in the effective thermal conductivity of the packed bed adsorber.

Acknowledgements

The authors gratefully acknowledge the financial support of the Natural Sciences and Engineering Research Council of Canada (NSERC) through the Automotive Partnership Canada Grant No. APCPJ 401826-10. We thank Dr. Wendell Huttema from LAEC for valuable discussion.

Appendix A

The equations which are used in the present model to find the micro/macro-contact and micro/macro-gap resistances are listed in Table A1 (for more details, see Refs. [28,29,42]).

References

[1] D. Ürge-Vorsatz, L.F. Cabeza, S. Serrano, C. Barreneche, K. Petrichenko, Heating and cooling energy trends and drivers in buildings, Renew. Sustain. Energy Rev. 41 (2015) 85–98.

[2] K.F. Fong, T.T. Chow, C.K. Lee, Z. Lin, L.S. Chan, Comparative study of different solar cooling systems for buildings in subtropical city, Sol. Energy 84 (2) (2010) 227–244.

[3] N. Yu, R.Z. Wang, L.W. Wang, Sorption thermal storage for solar energy, Prog. Energy Combust. Sci. 39 (5) (2013) 489–514.

[4] L.F. Cabeza, Advances in Thermal Energy Storage Systems: Methods and Applications, Woodhead Publishing, 2014.

[5] Y.I. Aristov, I.S. Glaznev, I.S. Girnik, Optimization of adsorption dynamics in adsorptive chillers: Loose grains configuration, Energy 46 (1) (2012) 484–492.

[6] I.I. El-Sharkawy, H. Abdelmeguid, B.B. Saha, Towards an optimal performance of adsorption chillers: Reallocation of adsorption/desorption cycle times, Int. J. Heat Mass Transf. 63 (2013) 171–182.

[7] L. Pistocchini, S. Garone, M. Motta, Air dehumidification by cooled adsorption in silica gel grains. Part I: Experimental development of a prototype, Appl. Therm. Eng. 107 (2016) 888–897.

[8] A. Ramzy, K.T.P. Ashok Babu, R. Kadoli, Semi-analytical method for heat and moisture transfer in packed bed of silica gel, Int. J. Heat Mass Transf. 54 (4) (2011) 983–993.

[9] A. Hauer, F. Fischer, Open adsorption system for an energy efficient dishwasher, Chem. Ing. Tech. 83 (1–2) (2011) 61–66.

[10] V. Palomba, S. Vasta, A. Freni, Experimental testing of AQSOA FAM Z02/water adsorption system for heat and cold storage, Appl. Therm. Eng. 124 (2017) 967–974.

[11] A. Freni, L. Bonaccorsi, L. Calabrese, A. Caprì, A. Frazzica, A. Sapienza, SAPO-34 coated adsorbent heat exchanger for adsorption chillers, Appl. Therm. Eng. 82 (2015) 1–7.

[12] K.E. N'Tsoukpoe, G. Restuccia, T. Schmidt, X. Py, The size of sorbents in low pressure sorption or thermochemical energy storage processes, Energy 77 (2014) 983–998.

[13] A. Rezk, R.K. Al-Dadah, S. Mahmoud, A. Elsayed, Effects of contact resistance and metal additives in finned-tube adsorbent beds on the performance of silica gel/water adsorption chiller, Appl. Therm. Eng. 53 (2) (2013) 278–284.

[14] X.H. Li, X.H. Hou, X. Zhang, Z.X. Yuan, A review on development of adsorption cooling - Novel beds and advanced cycles, Energy Convers. Manage. 94 (2015) 221–232.

[15] A. Sharafian, K. Fayazmanesh, C. McCague, M. Bahrami, Thermal conductivity and contact resistance of mesoporous silica gel adsorbents bound with polyvinylpyrrolidone in contact with a metallic substrate for adsorption cooling system applications, Int. J. Heat Mass Transf. 79 (2014) 64–71.
[16] D.B. Riffel, U. Wittstadt, F.P. Schmidt, T. Núñez, F.A. Belo, A.P.F. Leite, F. Ziegler, Transient modeling of an adsorber using finned-tube heat exchanger, Int. J. Heat Mass Transf. 53 (7–8) (2010) 1473–1482.
[17] A.R.M. Rezk, R.K. Al-Dadah, Physical and operating conditions effects on silica gel/water adsorption chiller performance, Appl. Energy 89 (1) (2012) 142–149.
[18] D. Zhu, S. Wang, Experimental investigation of contact resistance in adsorber of solar adsorption refrigeration, Sol. Energy 73 (3) (2002) 177–185.
[19] VDI Heat Atlas, second ed., Springer, 2010.
[20] A. Griesinger, K. Spindler, E. Hahne, Measurements and theoretical modelling of the effective thermal conductivity of zeolites, Int. J. Heat Mass Transf. 42 (23) (1999) 4363–4374.
[21] B. Dawoud, M.I. Sohel, A. Freni, S. Vasta, G. Restuccia, On the effective thermal conductivity of wetted zeolite under the working conditions of an adsorption chiller, Appl. Therm. Eng. 31 (14–15) (2011) 2241–2246.
[22] A.V. Luikov, A.G. Shashkov, L.L. Vasiliev, Y.E. Fraiman, Thermal conductivity of porous systems, Int. J. Heat Mass Transf. 11 (1968) 117–140.
[23] M.K. Sarwar, P. Majumdar, Thermal conductivity of wet composite porous media, Heat Recover. Syst. CHP 15 (4) (1995) 369–381.
[24] E. Tsotsas, H. Martin, Thermal conductivity of packed beds: a review, Chem. Eng. Process. 22 (1) (1987) 19–37.
[25] F.P. Incropera, D.P. Dewitt, T.L. Bergman, A.S. Lavine, Fundamentals of Heat and Mass Transfer, 2007.
[26] H. Czichos, T. Saito, L. Smith, Springer Handbook of Metrology and Testing, second ed., Springer, 2011.
[27] Yovanovich, Thermal spreading and contact resistances, in: A. Bejan, D. Kraus (Eds.), Heat Transfer Handbook, John Wiley and Sons Inc., New York, 2003.
[28] M. Bahrami, M.M. Yovanovich, J.R. Culham, Effective thermal conductivity of rough spherical packed beds, Int. J. Heat Mass Transf. 49 (19–20) (2006) 3691–3701.
[29] S. Song, M.M. Yovanovich, Correlation of thermal accommodation coefficient for engineering surfaces, in: Proceedings of the Twenty-fourth National Heat Transfer Conference and Exhibition, 1987, pp. 107–116.
[30] C.V. Madhusudana, Thermal Contact Conductance. Mechanical Engineering Series, second ed., Springer, 2014.
[31] S. Kayal, S. Baichuan, B.B. Saha, Adsorption characteristics of AQSOA zeolites and water for adsorption chillers, Int. J. Heat Mass Transf. 92 (2016) 1120–1127.
[32] K. Okamoto, M. Teduka, T. Nakano, S. Kubokawa, H. Kakiuchi, The development of AQSOA water vapor adsorbent and AQSOA coated heat exchanger, in: The International Sorption Heat Pump Conference 2011, 2010.
[33] H. Kakiuchi, M. Iwade, S. Shimooka, K. Ooshima, Novel zeolite adsorbents and their application for AHP and Desiccant system, IEA-Annex, 2005.
[34] H. Wei, A. Benjamin Teo, Chakraborty, W. Fan, Improved adsorption characteristics data for AQSOA types zeolites and water systems under static and dynamic conditions, Microporous Mesoporous Mater., 242, 2017, pp. 109–117.
[35] D. Stroud, The effective medium approximations: some recent developments, Superlattices Microstruct. 23 (3) (1998) 567–573.
[36] M. Kaviany, Principles of Heat Transfer in Porous Media, second ed., 1995.
[37] C.L. Tien, K. Vafai, Statistical upper and lower bounds of effective thermal conductivity of fibrous insulation, in: 2nd AIAA/ASME Thermophysics and Heat Transfer Conference, 1978.
[38] P. Karayacoubian, M. Bahrami, J.R. Culham, Asymptotic solutions of effective thermal conductivity, in: 2005 ASME International Mechanical Engineering Congress and Exposition, 2005.
[39] D.D. Do, Adsorption Analysis: Equilibria and Kinetics, Imperial College Press, 1998.
[40] M. Rouhani, W. Huttema, M. Bahrami, Effective thermal conductivity of packed bed adsorbers: Part 1 Experimental study, Int. J. Heat Mass Transf. 123 (2018) 1204–1211, https://doi.org/10.1016/j.ijheatmasstransfer.2018.01.142.
[41] I.S. Girnik, Y.I. Aristov, Dynamic optimization of adsorptive chillers: the 'AQSOA™-FAM-Z02 – Water' working pair, Energy 106 (2016) 13–22.
[42] M. Bahrami, J.R. Culham, M.M. Yananovich, G.E. Schneider, Review of thermal joint resistance models for nonconforming rough surfaces, Appl. Mech. Rev. 59 (1) (2006) 1.